In situ NO abatement by photocatalysis – study under continuous NO injection in a 10-m3 experimental chamber

Jivko Topalov, Julie Hot, Erick Ringot, Alexandra Bertron

In situ NO abatement by photocatalysis – study under continuous NO injection in a 10-m^3 experimental chamber

Jivko Topalov[a], *Julie Hot*[a*], *Erick Ringot*[a,b], *Alexandra Bertron*[a]

[a]LMDC, Université de Toulouse, INSA/UPS Génie Civil, 135 Avenue de Rangueil, 31077 Toulouse, Cedex 04 France.

[b]LRVision SARL, ZI de Vic, 13 Rue du Développement, 31320 Castanet-Tolosan, France.

*Corresponding author: Dr. Julie Hot, hot@insa-toulouse.fr

Abstract

Air pollution is a serious public health concern in France and many other countries. Nitrogen oxides (NO_x) include nitrogen monoxide (NO) and nitrogen dioxide (NO_2). They are mainly outdoor pollutants produced during combustion of fossil fuel. These gases can easily infiltrate buildings and thus increase indoor pollution. The recommended guideline values for NO_2 are 200 µg/m^3 (short-term exposure) and 40 µg/m^3 (long-term exposure). Although no guideline values exist for NO, this gas can be oxidized by atmospheric ozone and thus produce NO_2. This paper studies the depollution efficiency of photocatalysis towards indoor NO. Experiments were conducted at real scale, in a 10-m^3 experimental chamber developed at the LMDC and used as a reactor. The interior walls of the chamber were equipped with painted plasterboards treated with photocatalytic coating (3 g/m^2 of TiO_2). Gas was continuously injected into the chamber according to a specific procedure: (1) pollutant injection at high flow rate to reach 200 ppb of NO, (2) pollutant injection at low flow rate in order to keep the NO concentration constant at 200±10 ppb, and (3) photocatalysis activation by switching on the light. Typical indoor lighting systems (fluorescent tubes, LED and halogen bulbs) were tested and UV fluorescent tubes were also used to optimise the photocatalytic efficiency. Results showed that NO indoor concentration was reduced by photocatalysis in real-world conditions. Significant NO degradation was obtained under visible light. In addition, using the experimental procedure presented in this paper, a new method for evaluating air depollution efficiency by photocatalysis at real scale is proposed.

Keywords: Photocatalysis, NO_x, in situ, experimental chamber, TiO_2, visible light, indoor air quality

Acknowledgments

The authors are grateful to CRISTAL for providing the photocatalytic products, to the Laplace laboratory for its expertise in spectroscopy, and to Bronkhorst for financing the equipment used for flow measurement and control.

1 Introduction

Improving air quality has been a major concern in industrial countries for some years (Solomon 2012; Li et al. 2016; World Health Organization 2016). A considerable number of studies have dealt with the subject from various points of view: socio-economic impacts (General & Kopp 2014), substances qualified as pollutants (Colls 2002), political decisions concerning air pollution reduction (Fenger 2009) and so on. Improvement of air quality has relied on two types of action: (1) limiting pollution production as much as possible by effective production control (EU 2008), and (2) using techniques to treat already existing air pollutants.

This paper focuses on nitrogen oxides (NO_x). This group of gaseous pollutants includes nitric oxide (NO) and nitrogen dioxide (NO_2). In urban areas, combustion processes release large amounts of NO_x, the main sources being traffic and industries. Indoors, NO_x are produced by chimneys, gas burners, cooking devices and tobacco smoke. Furthermore NO_x can infiltrate from outdoors (Blondeau et al. 2005). Since over 80% of our time is spent in an indoor environment (Klepeis et al. 2001), it is primordial to increase the understanding of indoor pollution, identify the types of pollutants, and evaluate, control and reduce their concentrations. Nowadays, guideline values exist to help public authorities to combat air pollution. They were established by organisations such as the World Health Organization (WHO) and the French Indoor Air Quality Observatory (OQAI) (Mosqueron & Nedellec 2005; World Health Organization 2006; Krzyzanowski & Cohen 2008; General & Kopp 2014). For example, NO_2 guideline values are: 200 $\mu g/m^3$ for short-term exposure and 40 $\mu g/m^3$ for long-term exposure. Limit values for NO have not been defined yet (Mosqueron & Nedellec 2004; Mosqueron & Nedellec 2005) even though NO and NO_2 concentrations are directly related. In fact, while most car exhaust systems produce mainly NO, part of it can react with the atmospheric ozone and form NO_2 (Mills & Elouali 2015).

For a few decades, photocatalysis has been put forward as a means to fight air pollution (Fujishima et al. 2000). Studies on the use of semi-conductors such as TiO_2 or ZnO are abundant in the literature (Fujishima et al. 2008; Yu & Brouwers 2009; Lin et al. 2013; Zhong & Haghighat 2015; Ren et al. 2017). Most experimental studies have been performed under laboratory conditions at different reactor scales (Horgnies et al. 2015; Toro et al. 2016a; Ifang et al. 2014; Horgnies et al. 2012; Ren et al. 2017; Martinez et al. 2011; Hot, Topalov et al. 2017; Hernández Rodríguez et al. 2016; Hüsken et al. 2009; Aïssa et al. 2011). Often, photocatalytic oxidation (PCO) efficiency is estimated using international standards and recommendations (ISO 22197-1 2016; CEN/TS 16980-1 2016). However, experiments carried out under such conditions are not very realistic representations of actual applications, where photocatalytic coatings are applied on large existing surfaces, and some authors have worked on this problem. Assessing PCO efficiency towards air pollution under real-world conditions is a tricky task and only a few studies on this subject have been published so far (Maggos et al. 2007; Maggos et al. 2008; Gallus et al. 2015; Hot, Martinez, et al. 2017; Chen & Chu 2011; Crain et al. 2016; Horgnies et al. 2015; Guerrini 2012). Moreover, only a handful of them are related to indoor air. In this paper, PCO of NO under real-world conditions is described, where “real-world conditions” should be understood as those existing in an actual house, built from common materials and enabling natural exchanges with the ambient environment. In the work reported here, a specific experimental procedure was used to evaluate the reduction of NO indoor concentration under different lighting systems over a few hours. Two different

methods are also proposed for evaluating photocatalytic depollution efficiency from available experimental data.

2 Materials and methods

2.1 Materials

2.1.1 Experimental house

The air depollution efficiency of photocatalytic materials towards NO was evaluated under real-world conditions by using a small experimental house designed by the LMDC (Laboratory of Materials and Durability of Constructions, UPS/INSA, Toulouse, France). A schematic representation and some photographs of this experimental house are shown in Figure 1.

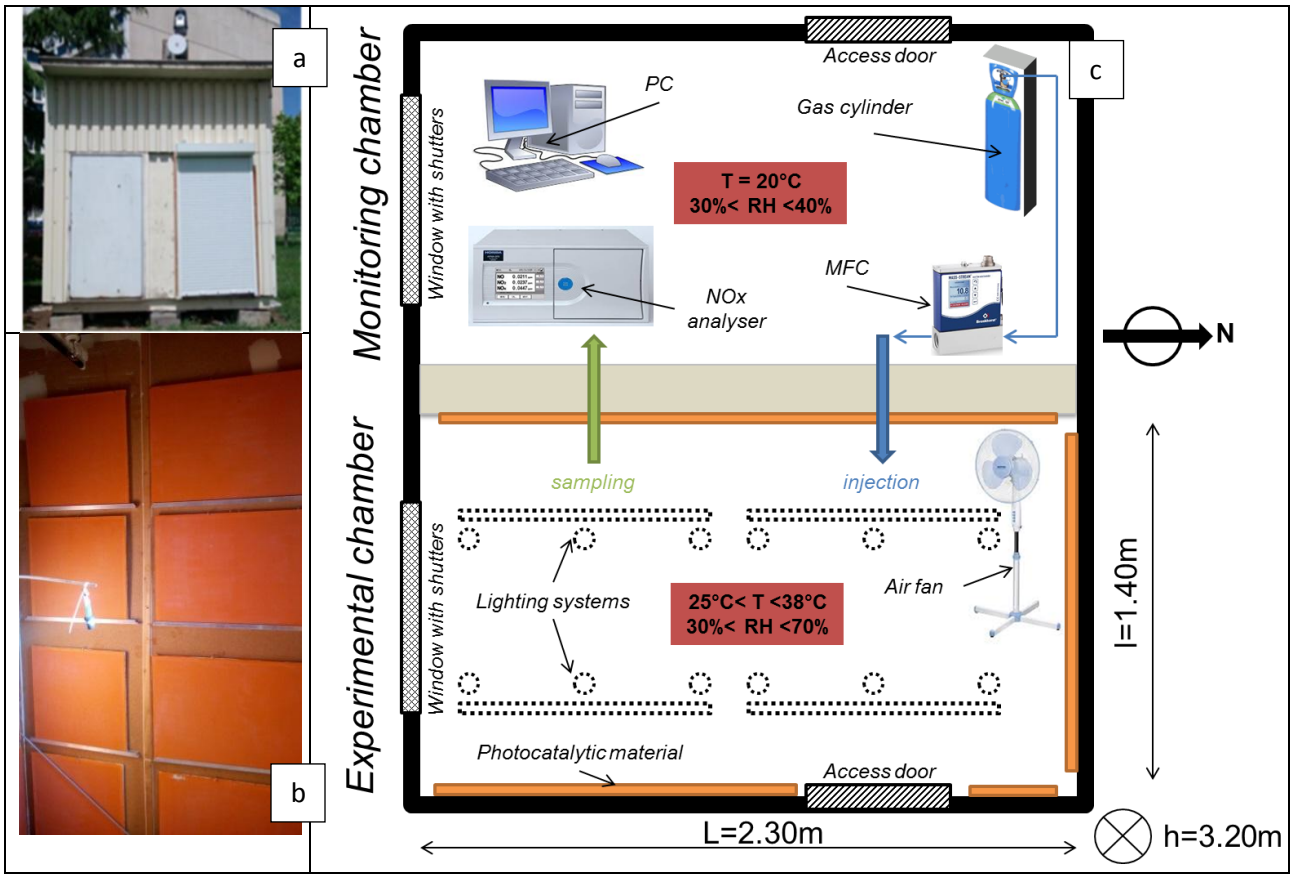

Figure 1 – Experimental house developed at the LMDC for photocatalytic assessment - (a) Outside view (South wall), (b) Photograph of the photocatalytic material (North wall), (c) Schematic representation of inside (viewed from above)

The isolated house was a simple metal framework structure composed of four walls, a rectangular floor and a flat roof. Inside, a wall divided the house into two chambers: (1) the experimental chamber (used as a photocatalytic reactor), and (2) the control chamber (used for equipment storage and experiment devices). The interior walls were covered by chipboard and each room had an external door and a

window. Two stainless tubes (6 mm in diameter) connected the chambers through the internal wall: one was used for gaseous pollutant injection, the other for air sampling.

The experimental chamber (roughly 10 m^3) was used as a vast photocatalytic reactor. Gaseous pollution was injected into it from the control chamber and was then diluted with indoor air. Some of this air was sampled. The experimental chamber was equipped with an air fan to improve pollution homogenisation and repeatability. No other mechanical ventilation was installed and the door and window were kept closed. However, indoor/outdoor exchanges occurred due to natural leakage. Thus, a standardised air tightness test was conducted (NF EN ISO 9972 2016). For an overpressure and underpressure of 4 Pa, total air leakage was 33-37 $m^3.h^{-1}$ and, for 50 Pa, leakage was 160-180 $m^3.h^{-1}$.The $Q4_{Pa\text{-}surf}$, which is the main indicator of air-tightness, was 1.32-1.44 $m^3.h^{-1}.m^{-2}$. The experimental chamber was therefore qualified as class D (A being the best and E the worst). This chamber was designed to assess photocatalytic activity occurring on the walls. Rather than treating existing interior wall surfaces directly, we applied the photocatalyst to removable plasterboards covering the walls, which enabled various photocatalytic materials to be tested. Aluminium U profiles were fixed on the internal walls to allow plasterboard plates be mounted and removed easily. On the ceiling, artificial lighting systems were installed to test various illumination conditions. Window shutters were kept closed to ensure that there was no interference with natural light and to allow tests to be carried out in the dark without activating the photocatalytic material. Temperature, relative humidity and indoor/outdoor pressure variations were not controlled (see Figure 1c); these parameters were influenced by the weather conditions and were constantly measured by probes (KIMO). During tests, the interior of the experimental chamber could be observed from the monitoring chamber via a camera.

The monitoring chamber was used to supervise experiments. As can be seen in Figure 1c, a gas cylinder (Air Liquide – 45 ppm of NO stabilised in N_2) was connected to a mass flow controller (MFC from M+W Instrumentation). The flow rate of pollution was thus controlled before its injection into the experimental chamber through the first stainless tube. Using the second stainless tube, polluted air was sampled at 1 ln/min without affecting the pollution level inside the experimental chamber. A NO_x analyser (HORIBA APNA-370) in the monitoring chamber measured NO_x (NO and NO_2) concentrations in the sampled air. This apparatus gave instantaneous results and enabled continuous monitoring and recording (one mean value every 5 min). The analyser was connected to a PC to store data and the evolution of pollution was observed graphically in real time. A camera was also connected to the PC. To preserve equipment service life, temperature and relative humidity (RH) were controlled by air conditioning (20°C and 30-40% RH). Finally, artificial lighting was also switched on/off from the monitoring room.

2.1.2 Photocatalytic material

The photocatalytic material consisted of painted plasterboards (used as the substrate) coated with a TiO_2 aqueous solution (used as the photocatalyst). Standard plasterboards (Placoplatre® BA 13) were purchased and cut into pieces with specific dimensions to fit the indoor walls of the experimental chamber (100x50 cm^2, 75x50 cm^2, 50x50 cm^2 and 50x25 cm^2). The edges of each piece were covered with an adhesive tape. Then, each plasterboard plate was painted with orange water-based acrylic paint containing natural pigment (provided by LRVision Company). Two layers were applied to plasterboard

surfaces using a paint roller. The photocatalytic dispersion was prepared by diluting a water-based commercial product (CristalACTiV™ S5-300B, TiO_2 content: 18 wt%) to obtain an aqueous solution containing 6 wt% of dry TiO_2. Three layers of this dispersion were applied to the plasterboard surfaces with the help of a brush. The total quantity of TiO_2 (dry matter) on substrate surfaces was 2.9±0.1 g/m². This quantity was controlled and determined by weighing the recipient containing the TiO_2 dispersion and the brush before and after coating each plasterboard sample. The targeted value of 3 g/m² of photocatalytic product on the surface was chosen according to previous research work carried out by the same authors (Hot, Topalov et al. 2017). Finally, each photocatalytic plasterboard sample was mounted on the walls inside the experimental chamber. An area of 9.3 m² of plasterboards was used to cover about half of the total indoor surface (ceiling, floor, door and window excluded).

2.1.3 Lighting conditions

Photocatalysis requires light and its activity is strongly dependent on light wavelengths and intensities. As the literature shows, UV-A lighting systems with wavelengths between 370 and 380 nm are very suitable for TiO_2 activation (Rajeshwar 2007; Ohama & Van Gemert 2011; Gaya & Abdullah 2008; Mamaghani et al. 2017). However, these illumination conditions are very limited in indoor environments. The objective of this paper was to study PCO under real-world conditions, so experiments were carried out under typical indoor lighting conditions. Three different types of visible light lamps were used: (1) four fluorescent tubes (Sylvania Luxline T8, 30 W, 2400 lm), (2) twelve LED bulbs (GE Energy Smart, 40 W, 470 lm), and (3) twelve halogen bulbs (Lumipro Eco, 55 W, 630 lm). Experiments were also conducted under UV light provided by four fluorescent tubes (Narva Blacklight blue LT-T8, 30 W) to observe the results under optimal conditions. During an experiment, the light was controlled from the monitoring chamber. The lamps were turned on or off by switches and light amplitude (brightness) could be adjusted by a dimmer. Here, the dimmer was always set to its brightest position in order to obtain optimal illumination. Thus, in this study, lighting conditions were characterised by the type of lamp, its wavelength and the irradiation intensity on the plasterboard surfaces.

Light intensity was measured with a radiometer (Gigahertz-Optik X1.1 Optometer) equipped with two detectors: a UV-A detector for wavelengths between 315 and 400 nm (model UV-3717) and a visible detector for wavelengths between 400 and 800 nm (model RW-3703). Firstly, the light intensity received by the surface of the photocatalytic material was investigated. Measurements were made at around 100 selected points to map the light intensity distribution on the walls. The map obtained under UV, illustrated in Figure 2, shows that light was able to reach every corner of the photocatalytic material. However, its intensity was dependent on the distance from the light source and ranged from 50 mW/m² (at floor level, 3 m from source) to 2,000 mW/m² (at approximately 2 m height, 1 m from source). Furthermore, at the same heights, the light appeared to be quite evenly distributed over the three walls (slightly lower on the North wall), and it was thus possible to quantify the received irradiation using a single mean value. Therefore, each lighting condition was expressed by the mean intensity value obtained at three different heights. The results are summarised in Table 1. The intensities of visible wavelengths under UV light or UV wavelengths under visible light were negligible.

To get an idea of a typical indoor light magnitude, a prior measurement campaign was carried out at the LMDC. Three rooms were targeted (office, lab room and classroom). Inside each room, light intensity was

recorded at different times of day over several days. Detectors were placed at 100 cm from the floor and were not exposed to direct sunlight. Visible and UV light intensity were measured under a combination of natural and artificial lighting. More details can be found in Hot, Topalov et al. (2017).The lowest mean UV intensity was 50 mW/m² and the highest was 260 mW/m², depending on the room location and aspect. These values were slightly lower than the ones obtained in the experimental chamber. Concerning visible light intensity, the lowest and highest mean values were respectively 2,200 mW/m² and 7,680 mW/m²: much higher than the values in the experimental chamber (from 300 to 6,100 mW/m² depending on the kind of lamps used). This was mostly due to the absence of natural light in the experimental chamber. In all cases, the experimental lighting conditions tested were considered to be representative of indoor environments.

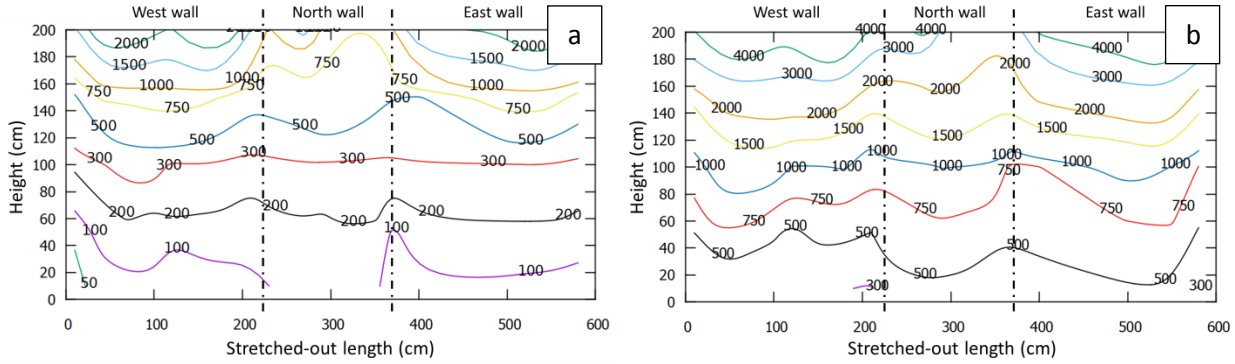

Figure 2 – Light mapping: irradiation received on photocatalytic material surfaces in the experimental chamber: (a) UV lighting system (in mW/m²), (b) Fluorescent lighting system (in mW/m²)

Table 1 – Mean light irradiation values received by photocatalytic material at different heights in the experimental chamber (in mW/m²)

	UV lighting 315<λ<400 nm	**Visible lighting 400<λ<800 nm**		
Height (cm)	Fluorescent	Fluorescent	LED	Halogen
20	40±20	400±100	300±100	900±100
100	300±50	1,000±200	800±200	1,700±300
180	1,200±300	2,500±500	2,300±300	6,100±500

According to the UV lamp data sheet, its distribution spectrum varies between 350 and 400 nm with a peak around 365 nm. In the case of visible lighting, the emission wavelengths of each system were investigated using a spectro-radiometer (Jeti specbos 1201) and the distribution spectrum of each lamp was obtained between 380 and 780 nm. The results are given in Figure 3. The fluorescent lamp showed a discontinuous spectrum with the luminous intensity focused on three major peaks: 436 nm, 544 nm and 612 nm. The halogen lamp had a rising, continuous spectrum with no dominant wavelengths. The LED lamp had a first peak around 450 nm and a second one around 605 nm, which were wider than the peaks of fluorescent light.

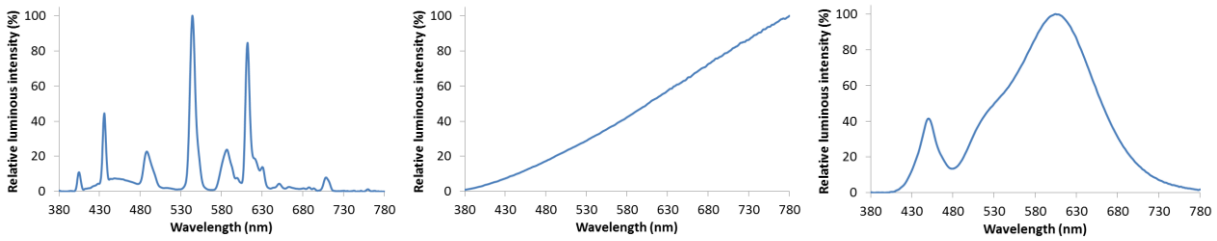

Figure 3 – Spectrum distribution between 380 and 780 nm: (a) Fluorescent, (b) Halogen, (c) LED

2.2 Experimental procedure

The experimental procedure consisted of injecting NO at a high flow rate until its concentration inside the experimental chamber reached 200 ppb. NO flow rate was then lowered to keep a constant level of pollution in the chamber (sufficient continuous NO injection to compensate for air leakage). PCO was then activated by switching on the light. The four steps listed below, illustrated in Figure 4, summarize this procedure:

Step 1: Background NO_x level assessment (30 min). Before NO pollutant injection, NO_x levels existing in the experimental chamber due to infiltration (outdoor pollution) were evaluated.

Step 2: NO injection until 200 ppb was reached (30 min). During this step, NO was injected at a high flow rate (1.5 ln/min for approximately 30 min) in order to reach 200 ppb of pollution inside the experimental chamber.

Step 3: NO concentration kept constant at 200 ppb (180 min). Once the concentration of 200 ppb was reached in the experimental chamber, the flow rate was lowered (0.3±0.02 ln/min) in order to maintain a constant NO pollution level over 180 min (± 2 ppb after 20 min and ± 10 ppb after 180 min).

Step 4: Photocatalysis activation (160 min). After observing pollution stability for 20 min, the light was switched on to activate photocatalysis. Depollution efficiency was evaluated with different lighting systems by following the NO concentration for up to 160 min.

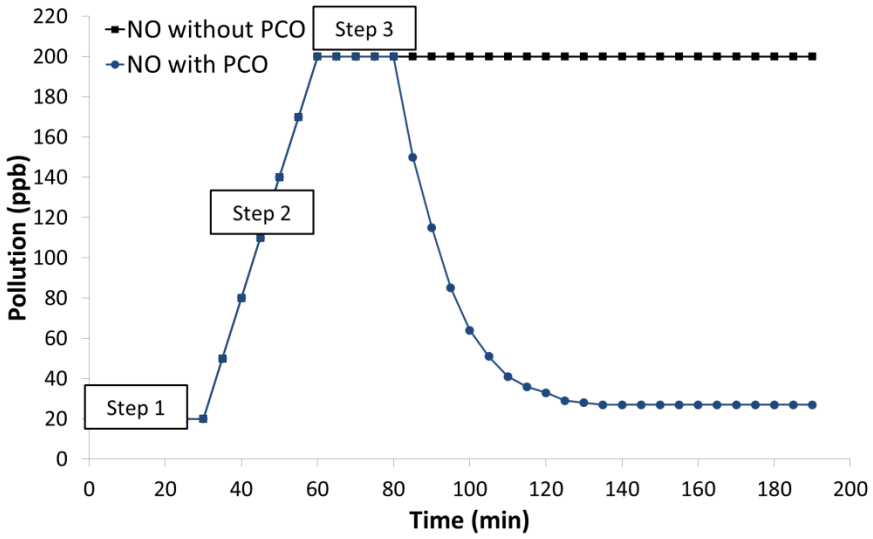

Figure 4 – A theoretical step by step diagram of the experimental procedure followed

In order to validate this experimental procedure, especially steps 2 and 3, a series of blank tests were first conducted in the dark (light OFF). For these tests, a constant pollution level was kept for more than 3h with a tolerance of ± 2 ppb after 20 min and ± 10 ppb after 180 min. In some cases, during the first few minutes of the pollution stabilisation step, it was necessary to adjust the flow rate (0.3±0.02 ln/min). Moreover, it was observed that maintaining a constant pollution level was harder on windy days. Photocatalytic tests were carried out three times to ensure a good repeatability.

3 Results and discussion

3.1 Background NO_x levels

The first step of the study was to collect data on NO_x background levels in the experimental chamber. As reported in the literature (Laurence 2015; Baukal 2005; Ao et al. 2003), NO_x are atmospheric gaseous pollutants that can easily infiltrate indoor air, so their levels and evolutions are strongly dependent on the surrounding environment. However, pollution levels also depend on the air exchange rate, which varies according to the building materials, insulation and ventilation (Blondeau et al. 2005). In this study, the NO_x analyser was used to monitor NO and NO_2 concentrations in outdoor air before the tests were carried out in the experimental chamber. The results revealed that outdoor air pollution was relatively low, probably because the experimental house was located on Toulouse university campus, surrounded by green spaces, far from boulevards and roadways.

Background pollution levels measured in the experimental chamber for a few days in March and April 2017 are illustrated in Figure 5. During March, pollution was relatively low and no peaks were observed for the 4-day period investigated. The background pollution level of NO_x was thus estimated from this measurement campaign: NO was between 10 and 20 ppb and NO_2 was below the analyser detection value of 3 ppb. During April, three NO peaks were observed in the 5 day investigation period: NO rose from a background level of 10-12 ppb to 50 ppb for the first peak and to 30 ppb for the other two. Each

peak lasted for a few hours. In contrast, NO_2 level remained under 3 ppb even when NO peaks appeared. Tests in the experimental chamber were thus carried out only if the NO initial background concentration (step 1) before injection was less than 30 ppb. Otherwise, tests were held over to a later date to ensure no initial pollution.

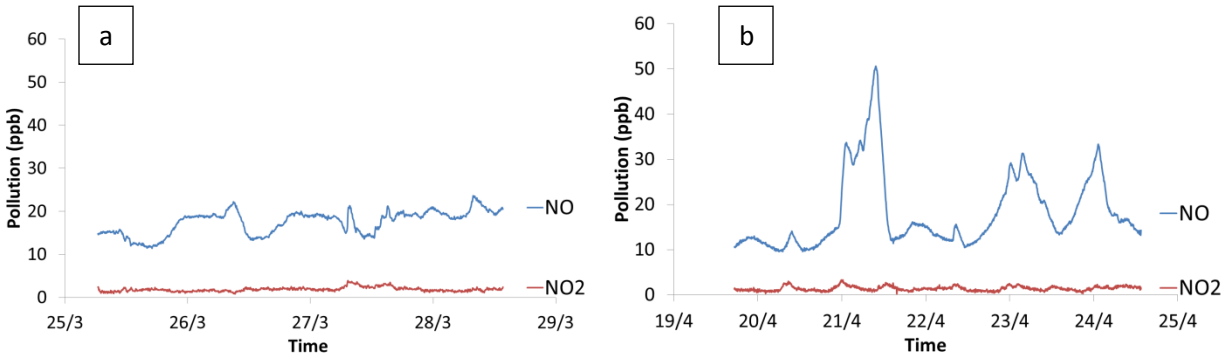

Figure 5 – NO_x concentrations in the experimental chamber coming from outdoor pollution - (a) 25-28 March 2017, (b) 20-24 April 2017

3.2 NO_x concentrations without photocatalysis

The second step was to continuously inject NO into the experimental chamber without light (light OFF) to ensure that a constant pollution level could be reached and maintained for at least 180 min. This blank test in the dark was conducted in the presence of photocatalytic plasterboards on the walls. In fact, no significant difference was noticed between tests carried out with and without photocatalytic material on the walls. This observation is in accordance with research work reported in the literature showing that NO has no adsorption properties (Maggos et al. 2007; Maggos et al. 2008; Hot, Martinez et al. 2017). The NO and NO_2 concentrations obtained over 240 min in the dark are given in Figure 6.

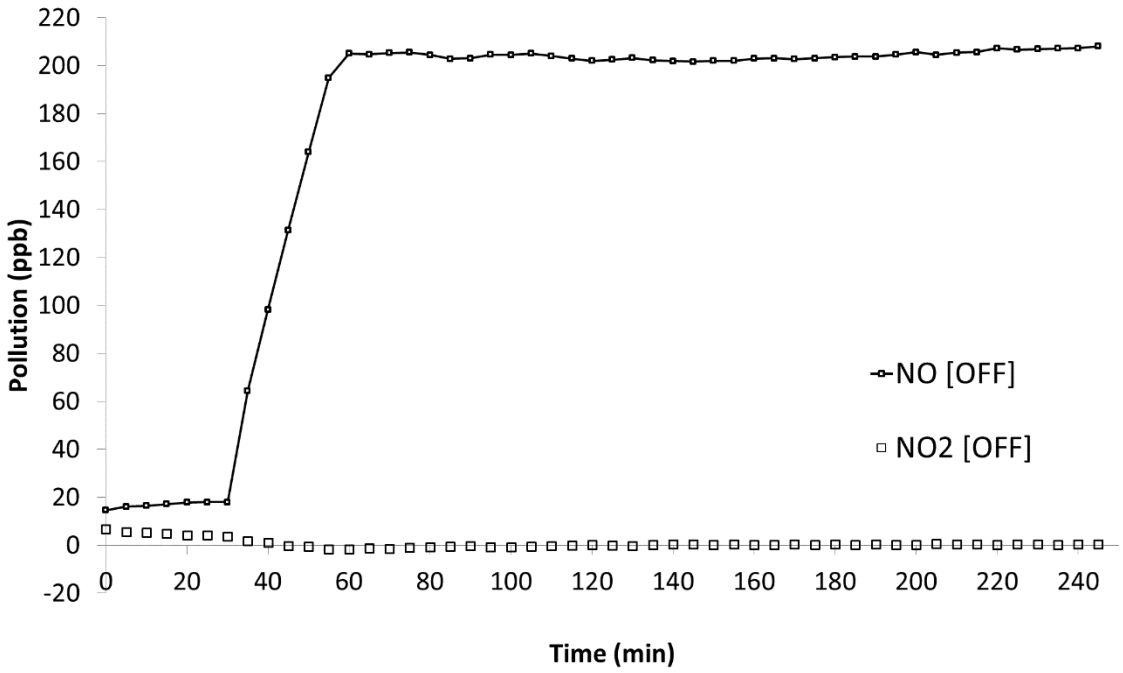

Figure 6 – Blank test: NO and NO_2 concentrations in the chamber in the dark before and during continuous NO injection

From t=0 min to t=30 min (step 1), NO_x concentration monitoring showed the expected NO and NO_2 background levels: around 15-20 ppb of NO and 0-5 ppb of NO_2. Starting at t=30 min, NO was continuously injected at 1.5 ln/min for about 28-30 min to reach 200 ppb (step 2). The pollution increased linearly, at a rate of 6.3±0.2 ppb/min. During this step, NO_2 concentration remained between 0 and 3 ppb. Just before 200 ppb was reached, the flow rate was lowered to 0.3 ln/min in order to maintain pollution at a constant level (step 3). NO pollution stabilized after only 5 min and lasted for 3 hours. Here again, NO_2 concentration remained low, (close to 0 ppb), which highlighted the absence of reaction between NO and NO_2 under these experimental conditions, especially in the dark. Therefore, steps 1 and 2 above allowed an NO concentration of 200 ppb to be reached rapidly in the experimental chamber and maintained it constant over 3 hours.

3.3 NO_x concentrations with photocatalysis

3.3.1 Under UV light

Figure 7 shows the variation of NO concentration in the experimental chamber when the UV light was switched on after step 2 (i.e. when NO pollution level had become constant).

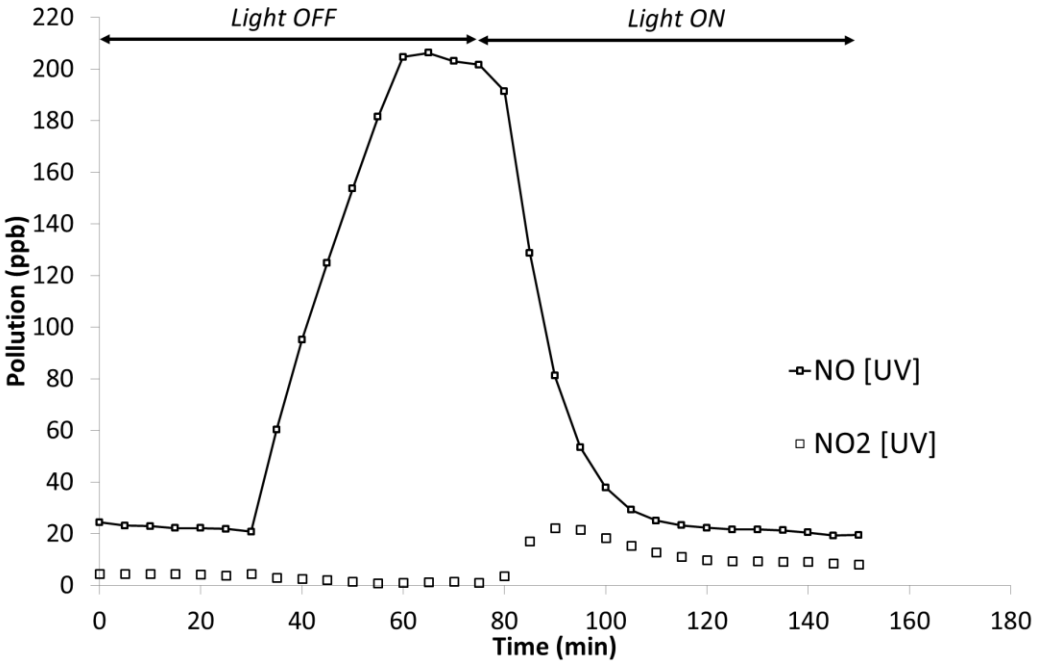

Figure 7 – NO photocatalytic degradation in the experimental chamber under UV light

Steps 1 and 2 were identical to the blank test conducted without light. After the pollution injection flow rate was lowered (at t=60 min), NO concentration was monitored in the dark for an extra 20 min to ensure it remained constant. At t=80 min, UV light was switched on to initiate photocatalytic oxidation. It can be seen in Figure 7 that, under UV light, photocatalysis had a significant depolluting effect with respect to NO. After only 20 min of photocatalytic activity (at t=100 min), NO concentration had fallen to 39.7 ppb. After 40 min (at t=120 min), the NO rate had returned to its minimum value, i.e. the background value (cf. part 3.1). The test was finally stopped after 70 min of UV illumination (at t=150 min) because NO and NO_2 concentrations remained constant.

Regarding NO_2, generation of this gas was observed during the first 10 min of photocatalytic activity (from t=80 min to t=90 min). While NO decreased from 200 to 80 ppb, NO_2 increased from 0 to about 20 ppb. Then, when the NO concentration stabilised at 20 ppb, NO_2 also decreased but remained at 8 ppb, which was higher than the background level (cf. part 3.1). Here, a mechanism of NO photocatalysis over TiO_2 is highlighted; NO_2 formed as a by-product at first but then some of it was destroyed. This observation is consistent with results reported by Hot, Martinez et al. (2017) in the case of NO static injection. More generally, NO_2 generation has always been observed in tests carried out at laboratory scale using photocatalytic reactor (Martinez et al. 2011; Martinez et al. 2013; Hot, Topalov et al. 2017; Karapati et al. 2014; Hernández Rodríguez et al. 2016; Crain et al. 2016; Ifang et al. 2014).

Results obtained in this study proved that our experimental chamber constituted a pertinent tool for assessing PCO at real scale and in real time. It was very remarkable that the entire injected NO was destroyed, showing that the depollution efficiency was almost 100% for the experimental conditions used here.

3.3.2 Under visible light

The photocatalytic degradation of NO under three visible lighting systems was assessed. The results are shown in Figure 8.

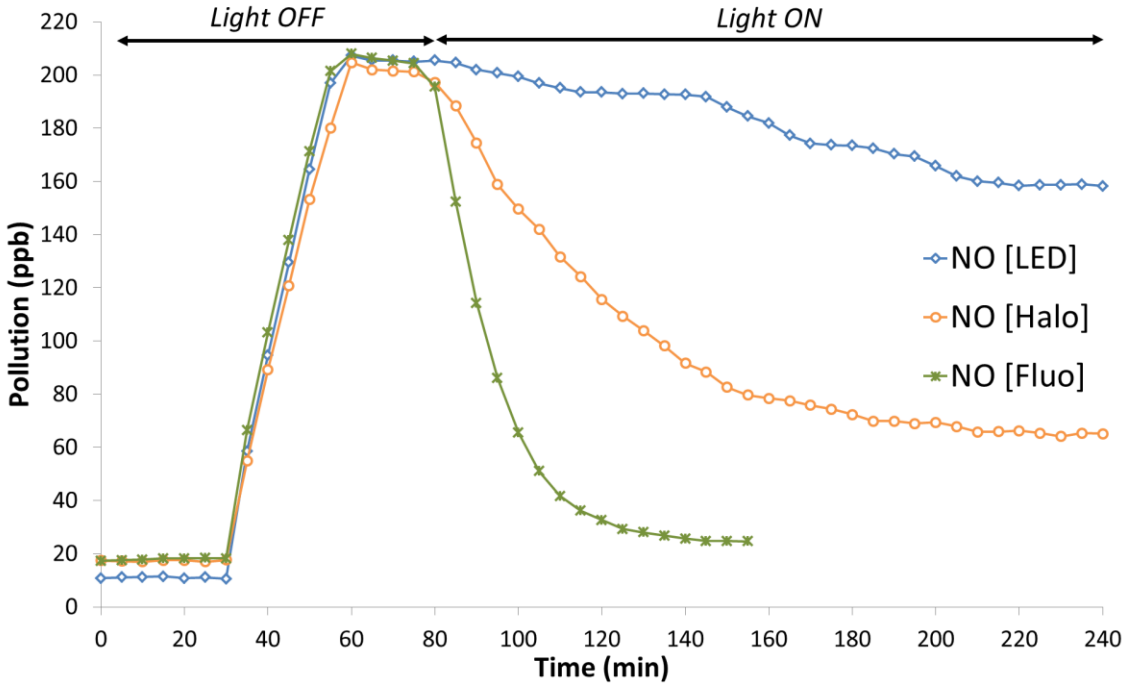

Figure 8 – Typical NO photocatalytic degradation in the experimental chamber under various visible lighting systems: Fluorescent, Halogen and LED

As expected, photocatalysis efficiency was dependent on the lighting systems used. The best photocatalytic degradation was obtained with fluorescent tubes. With this system, the NO concentration had fallen to 65.4 ppb after 20 min (at t=100 min) and the minimal value was reached after a further 50 min (at t=150 min). NO concentration remained constant and low, at a value around 25 ppb, which was slightly higher than the background pollution level. In this case, efficiency was nearly 98%. Halogen lamps led to lower degradation kinetics as the steady state was reached after 140 min of irradiation, with a final NO concentration of 64 ppb. Efficiency was thus around 78%. With LED used as lighting system, the photocatalytic activity was clearly less effective. In fact, NO concentration was around 159 ppb after 140 min of irradiation. The efficiency was only 22%. These results show that photocatalysis could be highly effective under visible light if a suitable lighting system was used. According to Table 1, halogen bulbs produced the highest light irradiation but the photocatalytic oxidation was not as effective as that observed with fluorescent tubes. In the case of LED, NO degradation was minimal although the light irradiation (intensity) was almost identical to that of fluorescent tubes. These results stress the influence of the light spectrum.

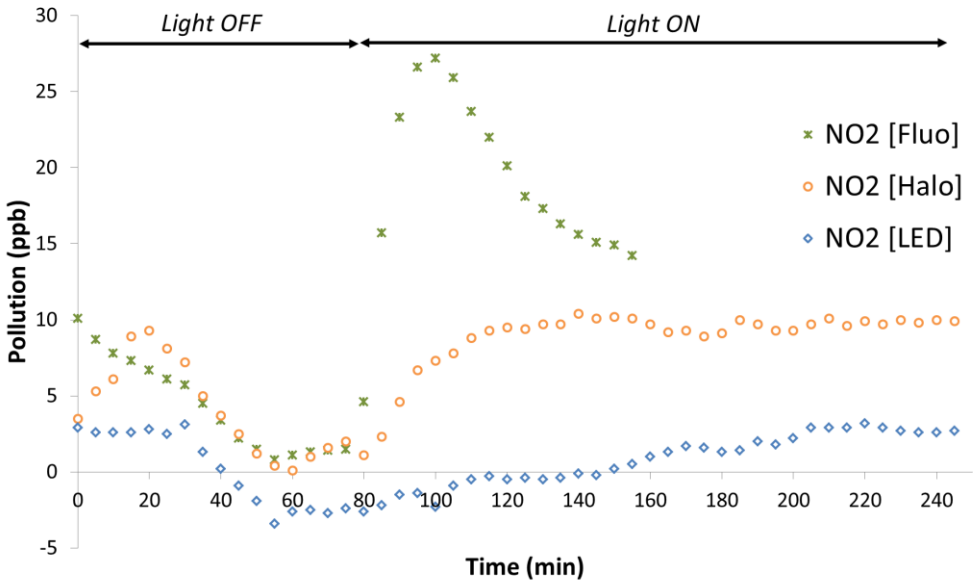

Figure 9 – NO_2 concentrations during NO oxidation by photocatalysis under different visible lighting systems: Fluorescent, Halogen and LED

Figure 9 shows NO_2 concentration variations obtained during tests carried out under visible light. NO_2 production was observed with fluorescent light. Because of the uncertainty on the NO_2 measurement (±5 ppb), the production of NO_2 under halogen and LED lamps was not clearly quantified. With visible fluorescent tubes, NO_2 production was maximal during the first 20 min of the photocatalytic reaction and then fell as has previously been observed with UV fluorescent tubes. With halogen and LED bulbs, NO_2 production lasted longer at a lower level.

3.4 Photocatalysis efficiency with respect to NO

NO photocatalytic depollution was assessed by two different methods. Firstly, the PCO slope and the lowest NO concentration values were determined as shown in Figure 9. The intersection of these two lines gave the time needed by the PCO to reach more than 85% of its maximum reaction efficiency. Secondly, the depollution rate was evaluated by comparing the quantity of NO obtained after PCO to the quantity without PCO (blank test).

3.4.1 PCO potential: slope & lowest NO level

The PCO potential was a method suggested by the authors to estimate the photocatalysis efficiency. This also allowed the efficiency of different lighting systems to be classified according to photoactivity. Two values were assessed: (1) the slope of NO decrease under PCO, and (2) the lowest NO concentration recorded after a maximum of 3 hours' illumination. The uncertainty on the slope was also estimated from the different measurements. Experiments were stopped earlier if a steady state was reached. The results are summarised in Table 2 and a graphical illustration of this method is given in Figure 10.

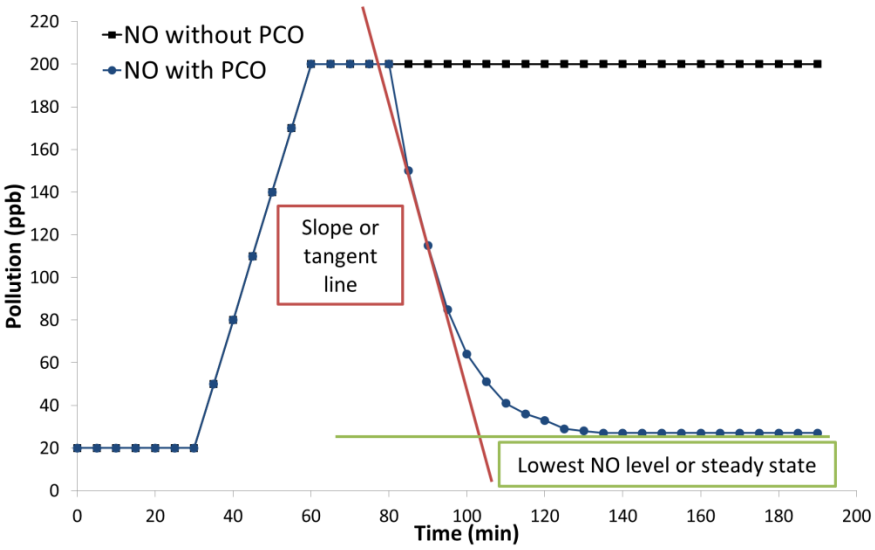

Figure 10 – Graphical illustration of PCO potential method

Table 2 – Values and uncertainties obtained to assess PCO potential under UV and visible light.

Lighting system	UV	Fluo	Halo	LED
Slope (ppb/min)	7.7±1.2	5.9±0.8	1.9±0.4	0.3±0.1
Lowest NO level (ppb)	20±5	25±5	64±5	160±5

3.4.2 PCO depollution rate

The PCO depollution rate was a second method suggested by the authors to evaluate photocatalysis efficiency. It consisted of assessing the mass of NO degraded by a square metre of photocatalytic material over a period of one minute. The mass of NO injected after t=80 min (light OFF) was first calculated for each test using equation (1):

$$M_{NO\ Blank} = M_{NO\ gc} * \frac{1}{V} * \phi * t \quad (1)$$

where $M_{NO\ Blank}$ is the mass of NO injected (in µg) during the blank test, $M_{NO\ gc}$ is the mass of NO in the gas cylinder (45 ppm or 55 215 µg/m^3), V is the chamber volume (10 m^3), ϕ is the injection flow rate (0.3 ln/min) and t is the injection time (min).

Then, the area under the blank test curve was calculated from t=80 min to the end of the test (A_{Blank}). In the same way, the area under each curve obtained with PCO was calculated (A_{PCO}). This allowed the area of NO removed ($A_{NO\ rem}$) - given in equation (2) and illustrated in Figure 11 - to be assessed.

$$A_{Blank} - A_{PCO} = A_{NO\ rem} \quad (2)$$

This area was used to determine the mass of NO removed ($M_{NO\ rem}$) according to equation (3).

$$M_{NO\ rem} = \frac{A_{NO\ rem}}{A_{blank}} * M_{NO\ Blank} \quad (3)$$

Finally, equation (4) was used to obtain the depollution rate, DR (µg.min^{-1}.m^{-2}). S_{PC} was the total area covered by the photocatalytic material (m²) and t_{PC} was the total time of light irradiation (min). Results are presented in Table 3.

$$DR = \frac{M_{NO\ removed}}{S_{PC} * t_{PC}} \quad (4)$$

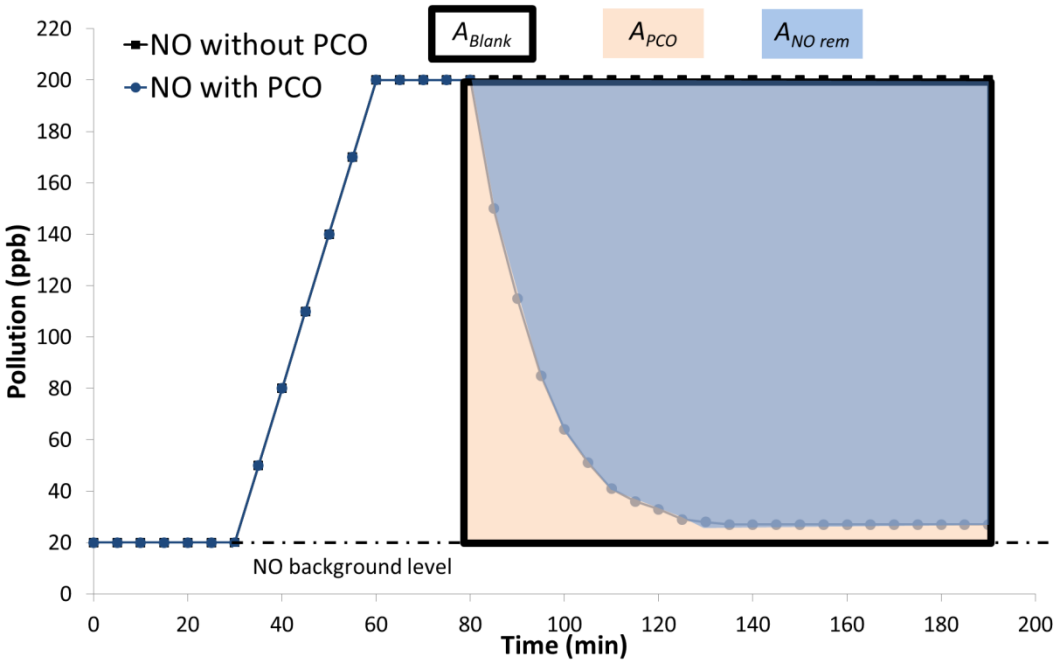

Figure 11 – Graphical illustration of PCO depollution rate method

Table 3 – Results obtained for PCO depollution rate calculation

Lighting system	mass of NO injected (after t=80min)	NO injection time (after t=80min)	NO mass removed	Depollution rate
UV	1 160 µg	70 min	1 100 µg	1.60 µg.min^{-1}.m^{-2}
Fluorescent	1 325 µg	80 min	1 230 µg	1.55 µg.min^{-1}.m^{-2}
Halogen	2 650 µg	160 min	1 700 µg	1.08 µg.min^{-1}.m^{-2}
LED	2 650 µg	160 min	400 µg	0.26 µg.min^{-1}.m^{-2}

A similar method was used by Maggos et al. to evaluate the depollution rate of a TiO_2 photocatalytic paint in a 917 m^3, artificially closed car park (Maggos et al. 2007). The paint contained 10% TiO_2 and was applied over the total surface area of the ceiling (322 m²). These authors reported a DR between 3 and 7.8 µg.min^{-1}.m^{-2} under UV light. A total of 20 UV lamps were used to provide 1 W/cm² on the surface of the photocatalytic material. However, the pollution was generated from the exhaust gases of a running vehicle and different pollutants were thus present simultaneously (NO_x, VOCs, CO, CO_2). Also, the NO concentrations tested were much higher (between 650 ppb and 1 300 ppb). Under these experimental

conditions, Maggos et al. estimated the global photocatalytic removal of NO at around 20%. This value is lower than the ones obtained in this study: almost 100% and more than 95% were respectively reached under UV and visible light provided by fluorescent tubes. Therefore, care is needed when dealing with DR as its value could be over- or under-estimated if other information, such as initial or final pollutant concentration (the lowest value reached), is not specified.

4 Conclusions

Studies aimed at assessing PCO efficiency are mainly conducted at laboratory scale using a reactor and most of them are inspired by ISO 22197. However, this standard is not suitable for real-world applications. For example, the controlled experimental conditions, such as the small reactor volume, the residence and contact time of the pollutant, or the lighting system (UV and high intensity), are not representative of tests in situ and cannot be simply extrapolated to a larger scale. In this paper, a new, simple method for assessing PCO of gaseous air pollutants under real-world conditions has been presented. The targeted pollutant was NO. Its degradation by photocatalysis was studied using a specific procedure in an experimental chamber developed at the LMDC. Various lighting systems were tested to compare PCO efficiency under UV and visible light. The results clearly showed that the lighting systems played an important role in the photocatalytic efficiency. Under UV, nearly 100 % of NO was removed by PCO. Moreover, this study highlighted the reduction of NO concentration under visible light, especially from fluorescent tubes. Results showed 97 % degradation under visible light from fluorescent tubes, 78 % under visible light from halogen bulbs and 30 % under visible light from LED bulbs. LED lighting is gaining in popularity because of its light output coupled with its low energy consumption. The abatement reaction rate with this lighting is lower than those obtained with other systems. Nevertheless, the abatement remains significant and could even be improved by doping the photocatalyst as shown by several authors (Zhou et al. 2007; Todorova et al. 2013; Hu et al. 2015).

The experimental procedure proposed here allowed PCO to be tested at larger scale, under realistic conditions, such as chamber volume, pollutant injection flow rate and lighting condition. In a future publication, the authors will propose a simple numerical model that describes the pollutant evolution observed during the different stages of the experiment. Then, an attempt will be made to link results obtained in this experimental chamber and in a reactor at a lab scale in order to suggest a numerical model able to predict real scale results from those found using a reactor.

5 References

Aïssa AH, Puzenat E, Plassais A, Herrmann JM, Haehnel C, Guillard C (2011) Characterization and photocatalytic performance in air of cementitious materials containing TiO2. Case study of formaldehyde removal. *Applied Catalysis B: Environmental*, 107(1–2), pp.1–8.

Ao CH, Lee SC, Mak CL, Chan LY (2003) Photodegradation of volatile organic compounds (VOCs) and NO for indoor air purification using TiO2: Promotion versus inhibition effect of NO. *Applied Catalysis B: Environmental*, 42(2), pp.119–129.

408 Baukal C (2005) Everything you need to know about NOx. *Metal Finishing*, 103(11), pp.18–24.

409 Blondeau P, Iordache V, Poupard O, Genin D, Allard F (2005) Relationship between outdoor and indoor
410 air quality in eight French schools. *Indoor Air*, 15(1), pp.2–12.

411 CEN/TS 16980-1 (2016) Photocatalysis - Continuous Flow Test Methods - Part 1: Determination Of The
412 Degradation Of Nitric Oxide (No) In The Air By Photocatalytic Materials. *EUROPEAN COMMITTEE*
413 *FOR STANDARDIZATION*.

414 Chen M, Chu JW (2011) NOx photocatalytic degradation on active concrete road surface - From
415 experiment to real-scale application. *Journal of Cleaner Production*, 19(11), pp.1266–1272.
416 Available at: http://dx.doi.org/10.1016/j.jclepro.2011.03.001.

417 Colls J (2002) *Air Pollution © 2002* 2nd Edition., London: Spoon Press.

418 Crain N, Juenger M, Cros C, Terpeluk A, Burris L, McDonald-Buller E, Sullivan D, Kimura Y, Spinhirne J,
419 Rung M (2016) Laboratory and Field Studies of Photocatalytic NOx and O3 Removal by Coatings on
420 Concrete - TECHNICAL REPORT 0-6636-1, Available at: http://library.ctr.utexas.edu/ctr-
421 publications/0-6636-1.pdf.

422 EU (2008) Directive 2008/50/EC of the European Parliament and of the Council of 21 May 2008 on
423 ambient air quality and cleaner air for Europe. *Official Journal of the European Communities*, 152,
424 pp.1–43.

425 Fenger J (2009) Air pollution in the last 50 years - From local to global. *Atmospheric Environment*, 43(1),
426 pp.13–22. Available at: http://dx.doi.org/10.1016/j.atmosenv.2008.09.061.

427 Fujishima A, Rao TN, Tryk DA, (2000) Titanium dioxide photocatalysis. *Journal of Photochemistry and*
428 *Photobiology C: Photochemistry Reviews*, 1(1), pp.1–21. Available at:
429 http://www.sciencedirect.com/science/article/pii/S1389556700000022.

430 Fujishima A, Zhang X, Tryk DA, (2008) TiO_2 photocatalysis and related surface phenomena. *Surface*
431 *Science Reports*, 63(12), pp.515–582.

432 Gallus M, Akylas V, Barmpas F, Beeldens A, Boonen E, Boréave A, Cazaunau M, Chen H, Daële V, Doussin
433 JF, Dupart Y, Gaimoz C, George C, Grosselin B, Herrmann H, Ifang S, Kurtenbach R, Maille M,
434 Mellouki A, Miet K, Mothes F, Moussiopoulos N, Poulain L, Rabe R, Zapf P, Kleffmann J (2015)
435 Photocatalytic de-pollution in the Leopold II tunnel in Brussels: NOx abatement results. *Building*
436 *and Environment*, 84(2), pp.125–133.

437 Gaya UI, Abdullah AH (2008) Heterogeneous photocatalytic degradation of organic contaminants over
438 titanium dioxide: A review of fundamentals, progress and problems. *Journal of Photochemistry and*
439 *Photobiology C: Photochemistry Reviews*, 9(1), pp.1–12. Available at:
440 http://linkinghub.elsevier.com/retrieve/pii/S1389556708000300.

441 General T, Kopp P (2014) ANSES Note and recommendations 2011-CRD-11 / Study of the socio-economic
442 cost of indoor air pollutants, Available at: https://www.anses.fr/en/documents/AUT-Ra-
443 CoutAirInterieurSHS2014-02EN.pdf.

444 Guerrini GL (2012) Photocatalytic performances in a city tunnel in Rome: NOx monitoring results.
445 *Construction and Building Materials*, 27(1), pp.165–175. Available at:

http://dx.doi.org/10.1016/j.conbuildmat.2011.07.065.

Hernández Rodríguez MJ, Pulido Melián E, González Díaz O, Araña J, Macías M, González Orive A, Doña Rodríguez JM (2016) Comparison of supported TiO_2 catalysts in the photocatalytic degradation of NOx. *Journal of Molecular Catalysis A: Chemical*, 413, pp.56–66.

Horgnies M, Dubois-Brugger I, Gartner EM (2012) NOx de-pollution by hardened concrete and the influence of activated charcoal additions. *Cement and Concrete Research*, 42(10), pp.1348–1355. Available at: http://dx.doi.org/10.1016/j.cemconres.2012.06.007.

Horgnies M, Dubois-Brugger I, Stora E (2015) An innovative de-polluting concrete doped with activated carbon to enhance air quality. In *10th International Concrete Sustainability Conference (NRMCA), At Miami (USA)*. pp. 0–13.

Hot J, Topalov J, Ringot E, Bertron A (2017) Investigation on parameters affecting the effectiveness of photocatalytic functional coatings to degrade NO : TiO_2 amount on surface, illumination and substrate roughness. *International Journal of Photoenergy*, pp.1–35.

Hot J, Martinez T, Wayser B, Ringot E, Bertron A (2017) Photocatalytic degradation of NO/NO2 gas injected into a 10-m3 experimental chamber. *Environmental Science and Pollution Research*, 24(14), pp.12562–12570. Available at: http://dx.doi.org/10.1007/s11356-016-7701-2.

Hu Y, Song X, Jiang S, Wei C (2015) Enhanced photocatalytic activity of Pt-doped TiO2 for NOxoxidation both under UV and visible light irradiation: A synergistic effect of lattice Pt4+and surface PtO. *Chemical Engineering Journal*, 274(x), pp.102–112. Available at: http://dx.doi.org/10.1016/j.cej.2015.03.135.

Hüsken G, Hunger M, Brouwers HJH (2009) Experimental study of photocatalytic concrete products for air purification. *Building and Environment*, 44(12), pp.2463–2474. Available at: http://dx.doi.org/10.1016/j.buildenv.2009.04.010.

Ifang S, Gallus M, Liedtke S, Kurtenbach R, Wiesen P, Kleffmann J (2014) Standardization methods for testing photo-catalytic air remediation materials: Problems and solution. *Atmospheric Environment*, 91, pp.154–161. Available at: http://dx.doi.org/10.1016/j.atmosenv.2014.04.001.

ISO 22197-1 (2016) Fine ceramics (advanced ceramics, advanced technical ceramics) - Test method for air-purification performance of semiconducting photocatalytic materials - Part 1: Removal of nitric oxide. *AFNOR*. Available at: www.afnor.org.

Karapati S, Giannakopoulou T, Todorova N, Boukos N, Antiohos S, Papageorgiou D, Chaniotakis E, Dimotikali D, Trapalis C (2014) TiO_2 functionalization for efficient NOx removal in photoactive cement. *Applied Surface Science*, 319(1), pp.29–36. Available at: http://dx.doi.org/10.1016/j.apsusc.2014.07.162.

Klepeis NE, Nelson WC, Ott WR, Robinson JP, Tsang AM, Switzer P, Behar JV, Hern SC, Engelmann WH (2001) The National Human Activity Pattern Survey (NHAPS): a resource for assessing exposure to environmental pollutants. *Journal of Exposure Analysis and Environmental Epidemiology*, 11(3), pp.231–252. Available at: http://www.nature.com/doifinder/10.1038/sj.jea.7500165.

Krzyzanowski M, Cohen A (2008) Update of WHO air quality guidelines. *Air Quality, Atmosphere and Health*, pp.7–13.

485 Laurence G (2015) *Traitement de l'air intérieur par photocatalyse. Performance et innocuité de systèmes*
486 *et matériaux - Rapport de recherche ADEME*,

487 Li Y, Henze DK, Jack D, Kinney PL (2016) The influence of air quality model resolution on health impact
488 assessment for fine particulate matter and its components. *Air Quality, Atmosphere and Health*,
489 pp.51–68.

490 Lin L, Chai Y, Zhao B, Wei W, He D, He B, Tang Q (2013) Photocatalytic oxidation for degradation of VOCs.
491 *Open Journal of Inorganic Chemistry*, 3(January), pp.14–25.

492 Maggos T, Bartzis JG, Liakou M, Gobin C (2007) Photocatalytic degradation of NOx gases using TiO_2-
493 containing paint: A real scale study. *Journal of Hazardous Materials*, 146(3), pp.668–673.

494 Maggos T, Plassais A, Bartzis JG, Vasilakos C, Moussiopoulos N, Bonafous L (2008) Photocatalytic
495 degradation of NOx in a pilot street canyon configuration using TiO_2-mortar panels. *Environmental*
496 *Monitoring and Assessment*, 136(1–3), pp.35–44.

497 Mamaghani AH, Haghighat F, Lee CS (2017) Photocatalytic oxidation technology for indoor environment
498 air purification: The state-of-the-art. *Applied Catalysis B: Environmental*, 203, pp.247–269. Available
499 at: http://dx.doi.org/10.1016/j.apcatb.2016.10.037.

500 Martinez T, Bertron A, Ringot E, Escadeillas G (2011) Degradation of NO using photocatalytic coatings
501 applied to different substrates. *Building and Environment*, 46(9), pp.1808–1816.

502 Martinez, T, Dompoint D, Bertron A, Escadeillas G (2013) Photocatalytic coatings for building materials:
503 degradation of NOx and inhibition of algal growth. I*nternational Journal of Restoration, Repair and*
504 *Renewal of Built Environment*, 4(1), pp.520–533.

505 Mills A, Elouali S (2015) The nitric oxide ISO photocatalytic reactor system: Measurement of NOx removal
506 activity and capacity. *Journal of Photochemistry and Photobiology A: Chemistry*, 305(x), pp.29–36.

507 Mosqueron L, Nedellec V (2004) Inventaire des données françaises sur la qualité de l'air à l'intérieur des
508 bâtiments : Actualisation des données sur la période 2001-2004. *Observatoire de la qualité de l'air*
509 *intérieur (OQAI)*, pp.1–61

510 Mosqueron L, Nedellec V (2005) Hiérarchisation sanitaire des paramètres d'intérêt pour l'observatoire
511 de la qualité de l'air intérieur : application aux phtalates, parafines chlorées à chaine courte,
512 organo-etains, alkyl phénols et retardateurs de flamme bromes. *CSTB*, pp.1–98.

513 NF EN ISO 9972 (2016) Thermal performance of buildings - Determination of air permeability of buildings
514 - Fan pressurization method. *AFNOR*. Available at: www.afnor.org.

515 Ohama Y, Van Gemert D (2011) *Applications of Titanium Dioxide Photocatalysis to Construction*
516 *Materials : State-of-the-Art Report of the RILEM Technical Committee 194-TDP* Y. Ohama & D. Van
517 Gemert, eds., Dordrecht: Springer Netherlands. Available at: http://link.springer.com/10.1007/978-
518 94-007-1297-3.

519 Rajeshwar K (2007) Fundamentals of Semiconductors Electrochemistry and Photoelectrochemistry.
520 *Encyclopedia of Electrochemistry*, pp.1–51.

521 Ren H, Koshy P, Chen WF, Qi S, Sorrell CC (2017) Photocatalytic materials and technologies for air
522 purification. *Journal of Hazardous Materials*, 325, pp.340–366. Available at:

http://dx.doi.org/10.1016/j.jhazmat.2016.08.072.

Solomon PA (2012) Introduction : special issue of air quality , atmosphere and health for air pollution and health : bridging the gap from sources-to-health outcomes. *Air Quality, Atmosphere and Health*, pp.3–8.

Todorova N, Vaimakis T, Petrakis D, Hishita S, Boukos N, Giannakopoulou T, Giannouri M, Antiohos S, Papageorgiou D, Chaniotakis E, Trapalis C (2013) N and N,S-doped TiO_2 photocatalysts and their activity in NOx oxidation. *Catalysis Today*, 209(2), pp.41–46. Available at: http://dx.doi.org/10.1016/j.cattod.2012.11.019.

Toro C, Jobson BT, Haselbach L, Shen S, Chung SH (2016) Photoactive roadways: Determination of CO, NO and VOC uptake coefficients and photolabile side product yields on TiO_2 treated asphalt and concrete. *Atmospheric Environment*, 139, pp.37–45.

World Health Organization (2006) WHO Air quality guidelines for particulate matter, ozone, nitrogen dioxide and sulfur dioxide: global update 2005: summary of risk assessment. *Geneva: World Health Organization*, pp.1–22. Available at: http://whqlibdoc.who.int/hq/2006/WHO_SDE_PHE_OEH_06.02_eng.pdf?ua=1.

World Health Organization (2016) Ambient Air Pollution: A global assessment of exposure and burden of disease. *World Health Organization*, pp.1–131. Available at: www.who.int.org.

Yu QL, Brouwers HJH (2009) Indoor air purification using heterogeneous photocatalytic oxidation. Part I: Experimental study. *Applied Catalysis B: Environmental*, 92(3–4), pp.454–461.

Zhong L, Haghighat F (2015) Photocatalytic air cleaners and materials technologies - Abilities and limitations. *Building and Environment*, 91, pp.191–203. Available at: http://dx.doi.org/10.1016/j.buildenv.2015.01.033.

Zhou L, Tan X, Zhao L, Sun M (2007) Photocatalytic oxidation of NOx over visible-light-responsive nitrogen-doped TiO_2. *Korean Journal of Chemical Engineering*, 24(6), pp.1017–1021.